Fabrication and characterization of solution-processed methanofullerene-based organic field-effect transistors

Th. B. Singh,[a] N. Marjanović, P. Stadler, M. Auinger, G. J. Matt, S. Günes, and N. S. Sariciftci
Linz Institute for Organic Solar Cells (LIOS), Physical Chemistry, Johannes Kepler University Linz, Altenberger Strasse 69, Linz A-4040, Austria

R. Schwödiauer and S. Bauer
Soft Matter Physics, Johannes Kepler University Linz, Altenberger Strasse 69, Linz A-4040, Austria

(Received 29 November 2004; accepted 26 February 2005; published online 12 April 2005)

The fabrication and characterization of high-mobility, *n*-channel organic field-effect transistors (OFET) based on methanofullerene [6,6]-phenyl C_{61}-butyric acid methyl ester using various organic insulators as gate dielectrics is presented. Gate dielectrics not only influence the morphology of the active semiconductor, but also the distribution of the localized states at the semiconductor-dielectric interface. Spin-coated organic dielectrics with very smooth surfaces provide a well-defined interface for the formation of high quality organic semiconductor films. The charge transport and mobility in these OFET devices strongly depend on the choice of the gate dielectric. The electron mobilities obtained are in the range of 0.05–0.2 $cm^2\,V^{-1}\,s^{-1}$. Most of the OFETs fabricated using organic dielectrics exhibit an inherent hysteresis due to charge trapping at the semiconductor-dielectric interface. Devices with a polymeric electret as gate dielectric show a very large and metastable hysteresis in its transfer characteristics. The observed hysteresis is found to be temperature dependent and has been used to develop a bistable memory element. © *2005 American Institute of Physics*. [DOI: 10.1063/1.1895466]

I. INTRODUCTION

Recently, organic-based electronics evolved with thin-film devices like displays,[1–3] sensors,[4] electronic labels,[5,6] ring oscillators,[7] and complementary integrated circuits. The basic structure of organic electronics is the organic field-effect transistor (OFET). A low-voltage-operated, pentacene-based OFET with a self-assembled monolayer as ultrathin gate insulator was demonstrated with a mobility in the range of 1–1.5 cm^2/Vs.[8,9] To fabricate a complementary integrated circuit, high-mobility *p*- and *n*-type materials are required. However, very few organic semiconductors are *n* type, with acceptable electron mobilities.[10] We have recently demonstrated *n*-channel OFETs using hot wall epitaxy grown C_{60} thin films with electron mobilities up to 1 cm^2/Vs.[11]

The overall performance of an OFET critically depends on the choice of the gate dielectric.[12,13] Recently, polymeric insulators have been considered as gate dielectrics.[13–18] These polymeric materials (i) can be solution processed, (ii) give smooth films on transparent glass and also on plastic substrates, (iii) are suitable for opto-electronics such as photo-responsive OFETs due to their high optical transparency, (iv) can be thermally stable with a relatively small thermal expansion coefficient, and (v) can possess rather high dielectric constants on the order of 10.[13–18] Detailed studies have shown that the first few monolayers of organic semiconductors are highly ordered, allowing a high mobility of field-induced charge carriers when grown on top of polymeric dielectrics,[16,18] a crucial advantage in field-effect devices. Furthermore, insulating polymers are technically relevant in OFETs since there is no more need of inorganic materials, thereby allowing uniform production technologies with all organic layers in OFETs.

OFETs with polymeric insulators as gate dielectric usually exhibit hysteresis in the transfer characteristics (source-drain current I_{ds} as a function of the gate voltage V_{gs}). One mechanism for the hysteresis is charge trapping and detrapping at the interface between the insulator and the semiconductor. The concept of "floating-gate-like" effects in OFETs was first proposed by Katz *et al.*[19] Among the commonly used organic-based dielectrics, polyvinyl alcohol (PVA), is also known as a charge electret.[20,21] The large hysteresis in OFETs using PVA as dielectric layers have been utilized in a nonvolatile organic transistor memory element.[22] Other "ferroelectric-like" polymers, such as nylon poly(m-xylylene adipamide) P(MXD6)[23] and poly(vinylidenefluoride-trifluoroethylene)P(VDF-TrFE),[24] were also employed in OFET memories. On the other hand, OFETs with surface-treated inorganic dielectrics exhibit negative threshold voltage shifts (bias stressing effects), assumed to be due to the trapping of charges in less mobile states located in the semiconductor.[25,26] Metal-insulator-organic-semiconductor (MIS) structures exhibit a sizable hysteresis due to mobile ions or trap-forming interfacial charges.[27,28] For all these reasons, the choice of the insulator becomes a crucial step in device fabrication. However, the exact origin of hysteresis in OFETs is not yet fully established.

In this paper we report on solution-processed top-contact *n*-channel OFETs with organic dielectric materials. Spin-coated organic dielectrics are prepared with a very smooth

[a]Author to whom correspondence should be addressed; electronic mail: birendra.singh@jku.at

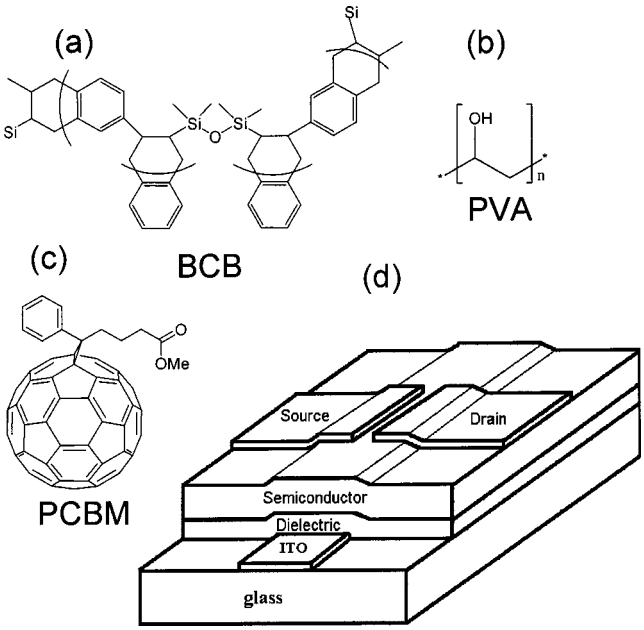

FIG. 1. Chemical structures of (a) divinyltetramethyldisiloxane-bis(benzocyclobutene) (BCB), (b) polyvinyl alcohol (PVA), (c) methanofullerene [6,6]-phenyl C_{61}-butyric acid methyl ester (PCBM), and (d) scheme of the top-contact OFET.

surface topology. Hence semiconducting films grown on top of the organic dielectric materials have a sharp interface resulting in electron mobilities as high as 0.2 cm^2/Vs in devices. The mobility of the devices scales with the dielectric constant of the gate dielectric. Depending on the choice of the dielectric, transistor performances with and without hysteresis are observed. The hysteresis is found to be strongly temperature dependent.

II. DEVICE FABRICATION

In this study, we have chosen three different dielectrics, viz., divinyltetramethyldisiloxane-bis(benzocyclobutane) (BCB), also known as "Cyclotene™" (Dow Chemicals), and two polyvinyl alcohols (PVA) (Mowiol® 40-88 and Fluka Chemicals). [6,6]-phenyl C_{61}-butyric acid methyl ester (PCBM) has been chosen as an *n*-type soluble organic semiconductor.[22] The molecular structures of the dielectrics and the organic semiconductor are shown in Figs. 1(a)–1(c). For comparison we have chosen two types of metals, Cr and LiF/Al, for the source-drain electrodes. A scheme of the device geometry is presented in Fig. 1(d). The device is fabricated on top of the ITO/glass substrate.

BCB was used as received from Dow Chemicals. BCB was spin coated at 1500 rpm from a 30% molar solution in mesitylene, yielding films with a thickness of 2 μm. After spincoating the BCB was thermally cross-linked for 30 min at 250 °C in an Ar atmosphere. Previous studies showed that BCB is an excellent dielectric material with a nearly temperature-independent thermal-expansion coefficient.[29] A 150 nm PCBM semiconducting layer was obtained by spin coating in an argon atmosphere (Ar) inside the glove box from a 3 wt % ratio chlorobenzene solution filtered with a 0.2-μm filter. The top source-drain electrodes, LiF/Al(0.6/60 nm) and Cr (20 nm), were evaporated under vacuum (3×10^{-6} mbars) through a shadow mask. Henceforth these devices are referred as device-$I_{LiF/Al}$ and device-I_{Cr}, with LiF/Al and Cr source-drain electrode, respectively.

Polyvinyl alcohol (PVA) (Mowiol® 40-88), with an average mol wt of 120,000 (Sigma-Aldrich), was spin coated at 1500 rpm from a 10% H_20 solution giving a thickness of around 3.8 μm. The rest of the device-fabrication procedure is identical to that described above for the BCB dielectric. We refer to these devices as device-$II_{LiF/Al}$ and device-II_{Cr}. PVA with an average mol wt of 100,000 (Fluka Chemicals) was used as a soluble gate electret. This PVA presumably contains a large number of mobile ions. Details of the device fabrication were described previously.[22] We refer to this device as device-III. Cr as a source-drain electrode was chosen because Cr does not significantly diffuse into the organic semiconductor layer. Similarly, LiF/Al was chosen since it is well known to form ohmic contacts with PCBM.[30,31] The electrical characterization of the devices was carried out in an Argon environment inside a glove box. Keithley 236 and Keithley 2400 instruments were employed for the steady-state measurements. For the temperature-dependent studies, the devices were transferred to a He-flow cryostat (Cryo Industries) using Lakeshore 331 as temperature controller without exposing the OFETs to air. The surface morphology and thickness of the dielectrics and the PCBM films on top of the dielectric materials were measured with a Digital Instrument 3100 atomic force microscopy and a DekTak Stylus profilometer.

III. RESULTS

As described above, the *n*-channel OFETs are based on the materials shown in Figs. 1(a)–1(c). Fig. 1(d) shows a scheme of our top-contact OFETs. The channel length L of the device is 60–70 μm and the channel width is $W = 1.4$ mm, giving a W/L ratio of 230. For better comparison four source-drain electrodes with different metals are evaporated on the same substrate. From the thickness of the dielectric and the capacitance per unit area C, the dielectric constant ε was obtained for all our devices. The results are summarized in Table I.

The film morphology of the three dielectrics is different, as revealed from atomic force microscopy (AFM) investigations shown in Figs. 2(a), 2(c), and 2(e). However, the surface roughness is only around 3.5 nm for all dielectrics employed. The Fluka PVA provided the smoothest surface among the dielectrics used in this study. A possible reason for the smoothness is the lyophilization and filtering of the Fluka PVA solution. In addition, filtered PCBM solutions also yielded very smooth films. Therefore very flat interfaces have been achieved favorable for the formation of highly conductive layers at the interface of the dielectric/PCBM. As shown in Figs. 2(b), 2(d), and 2(f), smooth PCBM films were also obtained with very good PCBM/metal interfaces.

The (I_{ds}-V_{ds}) plots for the device-$I_{LiF/Al}$ and device-$II_{LiF/Al}$ OFETs are shown in Figs. 3(a) and 3(b), respectively. With the same device dimensions, largely different I_{ds} values are obtained for the two devices. Hence we applied different gate voltages V_{gs} to observe sizable I_{ds} values (60 V to

TABLE I. Summary of the device parameters for PCBM OFETs with different dielectrics and source-drain electrode materials. The values shown here are an average of at least ten different devices fabricated under identical conditions.

Device	Dielectric	ε	C(nF/cm^2)	μ_c(cm^2 V^{-1} s^{-1})	V_t(V)	S(V/decade)	on/off ratio
Device-$I_{LiF/Al}$	BCB	2.6	1.2	0.07	2	8.4	1000
Device-I_{Cr}	BCB	2.6	1.2	0.05	7	7.31	2000
Device-$II_{LiF/Al}$	Mowiol® 40-88	8	1.8	0.2	−20	9.51	1000
Device-II_{Cr}	Mowiol® 40-88	8	1.8	0.1	−18	7.31	750
Device-III[a]	PVA(Fluka)	5	3	0.08	−14	7.45	3000

[a]Taken from Ref. 22.

device-$I_{LiF/Al}$ and 20 V to device-$II_{LiF/Al}$). Both devices feature rather high negative threshold *n*-channel FET in the electron accumulation mode with an applied positive V_{gs} and in the electron depletion mode with increasing negative V_{gs}. A saturated curve is obtained even at $V_{gs}=0$ V. A possible reason for such a feature is attributed to the presence of interface traps. The interface traps, rather than the doping of the semiconductor, are responsible for these effects. The presence of trap levels in the semiconductor lowers the conductivity of the material.[32] The "high negative threshold voltage" behavior is not related to the thickness of the dielectric. It should also be noted that these observations are in favor of the formation of highly conducting channels at the interface between the polymeric dielectric and the organic semiconductor.[16–18] Devices with Si-SiO_2 substrates treated with *n*-octadecyltrichlorosilane (OTS) were also found to be with high positive threshold.[12,13,33] The present results show a completely different transistor performance with the same semiconductor by choosing different organic dielectrics (Fig. 3). Devices with BCB (device-$I_{LiF/Al}$) show a very clear pinch-off voltage ($V_{ds} \geqslant V_{gs}$). This also implies a constant conductance under an applied V_{gs}. This kind of a transistor characteristic is best suited to calculate the intrinsic mobility μ of the semiconductor with a constant $I_{ds}(V_{ds}, V_{gs})$ in the saturated region using standard metal-oxide-semiconductor field-effect transistor (MOSFET) theory.[34] Devices with PVA (Mowiol® 40-88) (device-$II_{LiF/Al}$) exhibit 10^2 times higher current densities as compared to devices with BCB (device-$I_{LiF/Al}$) at the same V_{gs}. PVA (Mowiol® 40-88)-based devices give a nonideal $I_{ds}(V_{ds})$ with less well-defined pinch-off. A possible reason for such a characteristic is the presence of interface charges at the PVA (Mowiol® 40-88)/PCBM interface which lower the activation energy of free charge carriers due to the shift of the quasi-fermi level.[35,36] As seen in Fig. 3(b), $I_{ds}(V_{ds})$ exhibits a lower differential resistance above the pinch-off.

The dependence of the bulk current (also known as the "off-current") for the different dielectrics and source-drain electrodes is revealed in the transfer characteristics shown in Fig. 4(a). All the devices demonstrate a negligibly small hysteresis when V_{gs} is swept from −50 to +50 V and vice versa. It should be noted that PVA (Mowiol® 40-88)-based devices

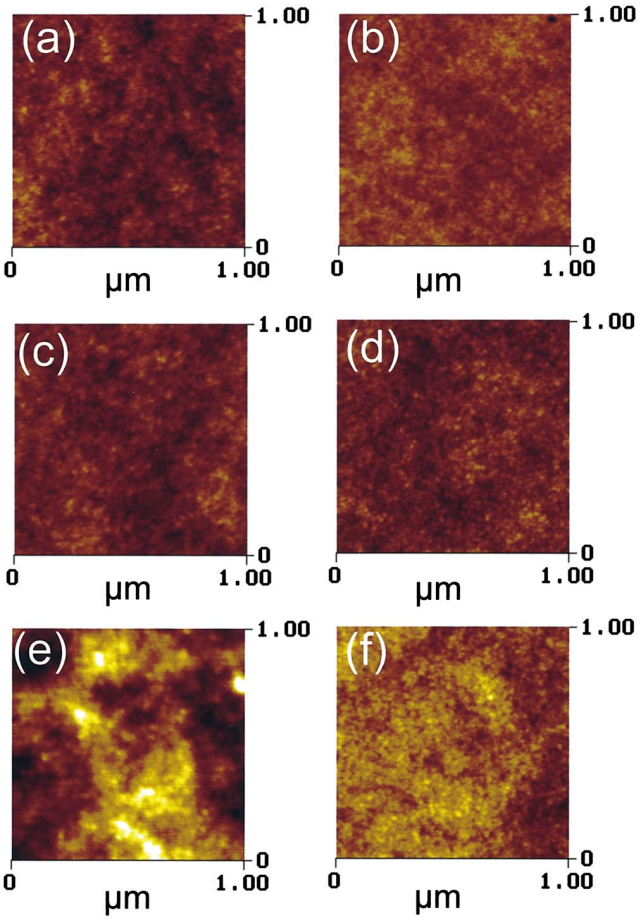

FIG. 2. Tapping mode AFM images of (a) BCB layer on ITO/glass, (b) PCBM film on top of the BCB/ITO/glass, (c) PVA (Mowiol® 40-88) layer on ITO/glass, (d) PCBM film on top of the Mowiol® 40-88/ITO/glass, (e) PVA (Fluka) layer on ITO/glass, and (f) PCBM film on top of the PVA (Fluka)/ITO/glass. All the images are taken with a height scale of 5 nm.

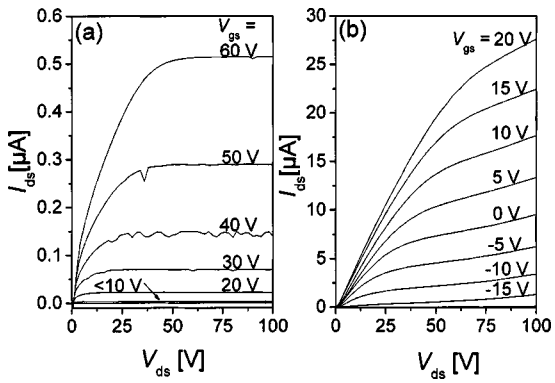

FIG. 3. (a) and (b) Transistor characteristics of device-$I_{LiF/Al}$ and device-$II_{LiF/Al}$, respectively, for different V_{gs}. All the measurements were carried out at room temperature. The data shown are taken in descending V_{gs} mode with an integration time of 1 s by averaging 10 points in steps of 2 V.

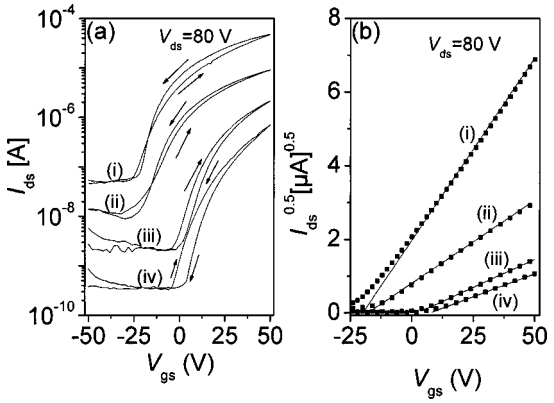

FIG. 4. (a) Transfer characteristics for (i) device-$II_{LiF/Al}$, (ii) device-II_{Cr}, (iii) device-$I_{LiF/Al}$, and (iv) device-I_{Cr}, demonstrating the different off-currents and directions of the hysteresis. The arrows indicate the direction of the V_{gs} sweep (b) $\sqrt{I_{ds}}$ versus V_{gs} plots for the data taken from the descending curves in Fig. 4(a) along with a theoretical fit using Eq. (1).

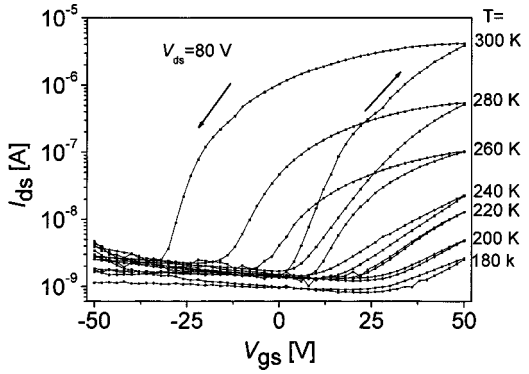

FIG. 5. Transfer characteristics for device-III—a bistable memory element with a strong temperature dependence of its the huge hysteresis. The arrows indicate the sweep direction of V_{gs}. Each measurement was carried out with an integration time of 1 s by averaging 10 points in steps of 2 V.

(device $II_{LiF/Al}$-II_{Cr}) and BCB-based devices (device $I_{LiF/Al}$-I_{Cr}) have a hysteresis in different directions. Therefore heating effects cannot be the origin of the observed hysteresis. Considering the difference of the two OFET devices with PVA (Mowiol® 40-88) and BCB as insulator, it is proposed that interface traps are responsible for these effects. Lowering of an order of magnitude in the off-current at $V_{gs}=0$ V is also observed when the LiF/Al source-drain electrode is replaced with Cr. This may be due to the smaller rate of diffusion of Cr into the organic semiconductor. All the devices have a quadratic I_{ds} dependence on V_{gs} as shown in Fig. 4(b). This allows us to calculate the mobility μ for all the devices using Eq. (1)[34]

$$I_{ds}=\frac{\mu WC}{2L}(V_{gs}-V_t)^2, \tag{1}$$

where V_t is the threshold voltage (defined as the gate-source voltage V_{gs}, where the free-charge carrier density equals the trap density).[32]

As shown in the plot of $\sqrt{I_{ds}}$ versus V_{gs}, [Fig. 4(b)], the slope for LiF/Al devices resulted in higher mobilities μ as compared to that for Cr. LiF is proposed to lower the barrier for electron injection from Al to the lowest unoccupied molecular orbital (LUMO) level of PCBM.[30,31] The lines in Fig. 4(b) are theoretical fits of the experimental data with Eq. (1). The theoretical curves fit well with the experimental curves, suggesting a constant mobility μ as a function of V_{gs} in the range of voltages investigated. Parameters calculated from the devices are summarized in Table I. The data presented in the table represents an average of at least 10 devices fabricated under identical conditions. The subthreshold slope S which determines the sharp turn in the behavior of the transistor is given by $S=dV_{gs}/d(\log I_{ds})$.[34] Usual OFETs have S in the range of 0.1–10 V/decade.[13,37] The present devices exhibit an S in the range of 8–9 V/decade due to the large thickness of the dielectric (see Table I). In addition, we also observed a sizable V_{ds}-dependent S (not shown here). Analogous to our findings, Scheinert *et al.*[37] presented a systematic study to clarify these peculiarities. Numerical simulations have been carried out with a systematic variation of the relevant material parameters and assuming the existence of interface or bulk trap states. In their studies, Scheinert *et al.* found that both the high S and its V_{ds} dependence can be explained by recharging of trap states either at the interface or in the bulk of the semiconductor.

The highest obtained mobility μ is 0.2 $cm^2\ V^{-1}\ s^{-1}$ from PVA (Mowiol® 40-88)-based devices (device $II_{LiF/Al}$-II_{Cr}), and the lowest mobility μ obtained is 0.05 $cm^2\ V^{-1}\ s^{-1}$ from BCB-based devices (device $I_{LiF/Al}$-I_{Cr}). As shown in Table I, μ is found to correlate with the dielectric constant ε of the dielectric. Our measured electron mobility μ is more than three orders higher than electron mobilities reported previously for PCBM-based OFETs with calcium (Ca) electrodes and poly(4-vinyl phenol) (PVP) as a dielectric in a similar device configuration.[38] A better device performance was obtained after sealing and storing the devices under ambient conditions in their studies. A very recent study showed ambipolar transport in PCBM-based transistors with SiO_2 as a dielectric, having a specific device structure where the source-drain electrode is ring type.[39] Their studies yielded an electron mobility $\mu=10^{-2}\ cm^2\ V^{-1}\ s^{-1}$ at $V_G=+20$ V. In their studies, the device characteristics were found to be strongly dependent on the annealing process and ambient conditions following the PCBM deposition. In addition, V_t was found to decrease from +25 V to $<+2$ V after annealing, while the measured electron mobilityincreased by more than two orders of magnitude. It was concluded that high vacuum, under which annealing was performed, was an essential process condition in order to obtain a good performance of their OFETs. It was observed that PCBM exhibits poor wetting behavior on $Si\text{-}SiO_2$ substrates resulting in rather smooth films. Upon annealing for several hours the PCBM films appear to be microcrystalline and rough. The authors attributed this drastic effect to the doping of the PCBM layer with ambient oxygen. The dopant sites act as electron traps that lead to a reduction in the number of mobile carriers and their mobility with a subsequent increase in V_t. Contrary to their results, our study show no detectable change in the device performance after annealing for 1 h at 120 °C in an inert argon (Ar) atmosphere inside the glove box. To the best of our knowledge, this is the highest electron mobility reported from a solution-processed *n*-type organic

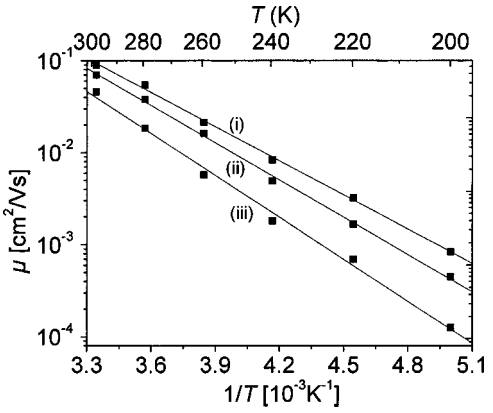

FIG. 6. Arrhenious plots for (i) device-III, (ii) device-$I_{LiF/Al}$, and (iii) device-I_{Cr}. The lines are Arrhenious fits to the experimental data.

semiconductors. We attribute this improvement in the device performance to the optimized film surface roughness, which provides a flat interface favorable for (i) excellent wetting properties of the organic dielectric substrate, (ii) the formation of highly conductive layers at the interface between the dielectric and PCBM, (iii) smooth interfaces between PCBM and the metal electrodes, and (iv) optimized electron-injection electrodes.

The origin of the hysteresis in the Fluka PVA electret gate dielectric is investigated through temperature (T)-dependent studies. As shown in Fig. 5, a very large hysteresis is observed under ambient conditions upon sweeping V_{gs}, as indicated by arrows.[22] The observed hysteresis is reduced upon cooling. Lowering the temperature, the process of charge trapping and detrapping is proposed to be frozen out, as usually observed in electrets. The nature of the charges are presumably ionic charges in the Fluka PVA. The activation energy E_a for the mobility is calculated by employing the Arrhenius formula ($\mu \propto \exp -\Delta E_a/kT$). The fit as shown in Fig. 6 reveals an activation energy of 100 meV for all the devices. The activation energy E_a reported here is in the same range to that found in PCBM diodes.[30] Therefore the activation energy E_a presented here is presumed to be an intrinsic property of the PCBM films independent of the kind of experiment performed for measuring μ.

IV. CONCLUSION

In conclusion, a detailed study of different *n*-channel OFETs based on PCBM, using various organic polymeric dielectrics, is presented. The device performance strongly depends on the choice of the dielectric. The inherent hysteresis in the transfer characteristics of these OFETs is strongly determined by the polymeric dielectric. Temperature-dependent studies show a freezing of the hysteresis, presumably due to the freezing of the trapping and the detrapping of charges at the interfaces. The mobilities μ obtained in this study is related to the dielectric constant ε of the gate dielectric.

Special thanks are due to V. N. Sivanandam for the lyophilization of the Fluka PVA. This work was performed within the Christian Doppler Society's dedicated laboratory on Plastic Solar Cells funded by the Christian Doppler Society and Konarka Austria GesmbH.

[1] J. A. Rogers *et al.*, Proc. Natl. Acad. Sci. U.S.A. **98**, 4835 (2001).
[2] H. E. A. Huitema *et al.*, Nature (London) **414**, 599 (2001).
[3] C. D. Sheraw *et al.*, Appl. Phys. Lett. **80**, 1088 (2002).
[4] B. K. Crone, A. Dodabalapur, R. Sarpeshkar, A. Gelperin, H. E. Katz, and Z. Bao, J. Appl. Phys. **91**, 10140 (2001).
[5] D. M. De Leew, G. H. Gelinck, T. C. T. Geuns, E. Van Veenendaal, E. Cantatore, and B. H. Huisman, Tech. Dig. - Int. Electron Devices Meet. **2002**, 293.
[6] P. F. Baude, D. A. Ender, M. A. Haase, T. W. Kelley, D. V. Muyres, and S. D. Theiss, Appl. Phys. Lett. **82**, 3964 (2003).
[7] H. Klauk, M. Halik, U. Zschieschang, F. Eder, G. Schmid, and Ch. Dehm, Appl. Phys. Lett. **82**, 4175 (2003).
[8] M. Halik *et al.*, Nature (London) **431**, 963 (2004).
[9] S. F. Nelson, Y.-Y. Lin, D. J. Gundlach, and T. N. Jackson, Appl. Phys. Lett. **72**, 1854 (1998).
[10] S. Kobayashi, T. Takenobu, S. Mori, A. Fujiwara, and Y. Iwasa, Appl. Phys. Lett. **82**, 458 (2003).
[11] Th. B. Singh *et al.*, Org. Electron. (in press).
[12] M. Shtein, J. Mapel, J. B. Benziger, and S. R. Forrest, Appl. Phys. Lett. **81**, 268 (2002).
[13] H. Klauk, M. Halik, U. Zschieschang, G. Schmid, W. Radlik, and W. Weber, J. Appl. Phys. **92**, 5259 (2002).
[14] R. Parashkov, E. Becker, G. Ginev, T. Riedl, H.-H. Johannes, and W. Kowalsky, J. Appl. Phys. **95**, 1594 (2004).
[15] J. Park, S. Y. Park, S. Shim, H. Kang, and H. H. Lee, Appl. Phys. Lett. **85**, 3283 (2004).
[16] F. Dinelli, M. Murgia, P. Levy, M. Cavallini, F. Biscarini, and D. M. de Leeuw, Phys. Rev. Lett. **92**, 116802 (2004).
[17] H. E. Katz, Ch. Kloc, V. Sunder, J. Zaumseil, A. L. Briseno, and Z. Bao, J. Mater. Res. **19** 1995 (2004).
[18] W. Michaelis, D. Wöhrle, and D. Schlettwein, J. Mater. Res. **19**, 2040 (2004).
[19] H. E. Katz, X. M. Hong, A. Dodabalapur, and R. Sarpeshkar, J. Appl. Phys. **91**, 1572 (2002).
[20] *Electrets*, edited by R. Gerhard-Multhaupt and G. M. Sessler (Laplacian, Morgan Hill, 1999), Vols. I and II.
[21] P. Frübing, M. Wegener, R. Gerhard-Multhaupt, A. Buchsteiner, W. Neumann, and L. Brehmer, Polymer **40**, 3413 (1999).
[22] Th. B. Singh, N. Marjanović, G. J. Matt, N. S. Sariciftci, R. Schwödiauer, and S. Bauer, Appl. Phys. Lett. **85**, 5409 (2004).
[23] R. Schroeder, L. A. Majewski, and M. Grell, Adv. Mater. (Weinheim, Ger.) **16**, 633 (2004).
[24] K. N. N. Unni, R. de Bettignies, S. Dabos-Seignon, J.-M. Nunzi, Appl. Phys. Lett. **85**, 1823 (2004).
[25] A. Sallelo, M. L. Chabinyc, M. S. Yang, and R. A. Street, Appl. Phys. Lett. **81**, 4383 (2002).
[26] S. Scheinert, G. Paaasch, S. Pohlmann, H. -H. Horhold, and R. Stockmann, Solid-State Electron. **44**, 845 (2000).
[27] E. J. Meijer, A. V. G. Mangnus, C. M. Hart, D. M. de Leeuw, and T. M. Klapwijk, Appl. Phys. Lett. **78**, 3902 (2001).
[28] S. Scheinert and W. Schliefke, Synth. Met. **139**, 503 (2003).
[29] R. Schwödiauer, G. S. Neugschwandtner, S. Bauer-Gogonea, S. Bauer, and W. Wirges, Appl. Phys. Lett. **75**, 3998 (1999).
[30] V. D. Mihailetchi *et al.*, Adv. Funct. Mater. **13**, 43 (2003).
[31] G. J. Matt, N. S. Sariciftci, and T. Fromherz, Appl. Phys. Lett. **84**, 1570 (2004).
[32] G. Horowitz, R. Hajlaoui, and F. Kouki, Eur. Phys. J.: Appl. Phys. **1**, 361 (1998).
[33] K. Shankar and T. N. Jackson, J. Mater. Res. **19**, 2003 (2004).
[34] S. M. Sze, *Physics of Semiconductor Devices* (Wiley, New York, 1981).
[35] M. A. Lampert and P. Mark, *Current Injection in Solids* (Academic, New York, 1970).
[36] S. Nešpůrek and J. Sworakowski, Radiat. Phys. Chem. **36**, 2 (1990).
[37] S. Scheinert, G. Paasch, M. Schrödner, H.-K. Roth, S. Sensfuß, and Th. Doll, J. Appl. Phys. **92**, 330 (2002).
[38] C. Waldauf, P. Schilinsky, M. Perisutti, J. Hauch, and C. J. Brabec, Adv. Mater. (Weinheim, Ger.) **15**, 2084 (2003); and private communications.
[39] T. D. Anthopoulos, C. Tanase, S. Setayesh, E. J. Meijer, J. C. Hummelen, P. W. M. Blom, and D. M. de Leeuw, Adv. Mater. (Weinheim, Ger.) **16**, 2174 (2004).